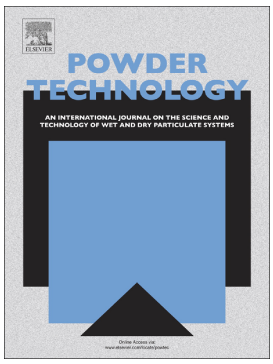

Oyster shell reuse: A particle engineering perspective for the use as emulsion stabilizers

Makrina A. Chairopoulou, Pablo Garcia-Triñanes, Ulrich Teipel

PII: S0032-5910(22)00614-3

DOI: https://doi.org/10.1016/j.powtec.2022.117721

Reference: PTEC 117721

To appear in: *Powder Technology*

Received date: 20 May 2022

Revised date: 23 June 2022

Accepted date: 11 July 2022

Please cite this article as: M.A. Chairopoulou, P. Garcia-Triñanes and U. Teipel, Oyster shell reuse: A particle engineering perspective for the use as emulsion stabilizers, *Powder Technology* (2022), https://doi.org/10.1016/j.powtec.2022.117721

Oyster shell reuse: A particle engineering perspective for the use as emulsion stabilisers

Makrina A. Chairopoulou[1,*] makrina.chairopoulou@th-nuernberg.de, Pablo Garcia-Triñanes[2], Ulrich Teipel[1,3]

[1]Department of Process Engineering, TH Nürnberg Georg Simon Ohm, Wassertorstr. 10, 90489 Nuremberg, Germany

[2]Materials and Chemical Engineering Group, School of Engineering, University of Greenwich, Medway, ME4 4TB, United Kingdom

[3]Department of Chemical Engineering, Ulm University, Ulm, Germany

[*]Corresponding author.

Abstract

Oyster shells are an important bioresource that causes serious environmental problems and is currently only partially repurposed. Its versatile nature is reflected in the manifold studies already proposed for the material. In this study, we add to this effort by first grinding the material with a hammer mill, beater disc mill, pin mill and wet media mill, treating part of it in a muffle furnace, noting the shift in its properties such as particle size, morphology, surface free energy, specific surface area and choosing a fraction to incorporate in a particle stabilized emulsion. The particle stabilized emulsions were prepared with oyster shells grinded by the agitated wet media mill at 2000 rpm for 30 min, with a media at x_{50}=0.72 µm, a SSA at 17.16 m^2/g, a SFE at 32.53 mN/m and with particles resembling a spherical shape. The emulsion was studied in terms of particle concentration, ranging from 2 – 10 wt% with the 8 wt% showing the best stability. The 8 wt% oyster shell formulation was tested and compared with a formulation using 2 wt% Aerosil particles and a surfactant store-bought product. The oyster shell particle formulation exhibited minor viscosity changes in the studied period of 8 weeks, a constant LVE range and promising behaviour in the proposed application.

Keywords: Oyster shells; Biomaterials; Recycling; Pickering emulsions; Particle engineering

List of symbols

τ_f	flow point [Pa]
τ_γ	yield point [Pa]
τ	shear stress [Pa]
x, x_{50}	size [µm]
G'	storage modulus
G''	loss modulus

Abbreviations and acronyms

BD	Beater disc
BOD	Biochemical oxygen demand
bOS	burned Oyster shells
COD	Chemical oxygen demand
FAO	Food and Agriculture Organization
HM	Hammer mill
LVE	Linear-viscoelastic range [Pa]
OS	Oyster shells

PD	Pin disc
SSA	Specific surface area
SFE	Surface free energy
TSS	Total suspended solids
uOS	unburned Oyster shells
WM	Agitated wet media mill

1. Introduction

Oysters are considered a delicacy by many and a silent killer by a few others (1). They are an ancient food and have been consumed around the World for tens of thousands of years. At first glance, oyster shells are considered a harmless residue since as a raw material they can slowly deteriorate naturally. Unfortunately, the substantial annual production quantities make this unrealistic. For the *Crassostrea gigas* species or commonly known as Pacific cupped oyster the FAO reported a world aquaculture production of 639,030 tons in 2017 (2) while for the American cupped oyster, *Crassostrea virginica* the global capture was estimated around 100,000 tons (3). The disposed shells are known to follow unbeneficial paths that both pollute the environment and waste a bioresource. Adult oyster shells of the *Crassostrea gigas* species, can contain up to 96 % $CaCO_3$ with the remaining 4 % being of an organic nature (4). As it was thoroughly described by *Lee et al.* oyster shells consist of multiple interchangeable layers of limestone and chalk (5). Depending on the species in question, in the front row of this struggle stand the biggest production sites such as China, Chile, South Korea, USA and Japan, while the problem mitigates along the food chain to every imported site as well.

Despite the many propositions that have been suggested for the versatile $CaCO_3$ (listed in **Section 2**) the problem still remains and requires further solutions. We here discuss the option of substituting surfactants in cosmetic formulations by $CaCO_3$ powder from oyster shells. The use of oyster shells as emulsifying aids in particle stabilized emulsions, or commonly known as Pickering emulsions, can offer distinct advantages. Studies around Pickering emulsions have seen a tremendous increase in recent years. The type of particles are chosen based on the internal phase and can vary from silica, carbon nanotubes, cellulose to different types of proteins and minerals (6).

The particles can be used as the prime stabilizer or as co-stabilizers to support the function of surfactants. Being larger than surfactants, particles can form a thicker barrier to shield the internal phase. Precipitated calcium carbonate has shown good results in stabilizing soybean oil in water in a O/W emulsion (7). *Huang et al.* studied various well-defined morphologies, such as rod, spheres and cubes, of precipitated calcium carbonate and demonstrated a higher stability of the rod like particles and the preference of the negatively charged oil phase to attract positively and preferentially small particles when exposed to a mixture of them.

To our knowledge calcium carbonate from oyster shells has not yet been studied in a Pickering emulsion system of this nature. The particles from oyster shells are retrieved by grinding the shells and thus have naturally a more randomized shape and morphology. Furthermore, the particles studied here are not treated at high temperatures or calcinated. This is important as the vast majority of uses for oyster shells require an energy intensive calcination step for the transformation of $CaCO_3$ in CaO. By preparing and testing oyster shells, we proposed in this study a viable alternative to the long list of solid materials appropriate for stabilizing emulsions.

Our focus is placed on the prerequisite treatment of the shells (**Section 3.2**), the particle characteristics such as morphology, charge and specific surface area (**Section 4.1**), the

incorporation of the powder in the formula (**Section 4.2**), and finally the aspect of formulation stability (**Section 4.3**). Through this, we propose an innovative solution to the oyster waste accumulation and landfill struggle while simultaneously offer an alternative to common surfactants in cosmetic applications.

2. Versatility of oyster shells

2.1.1 Water applications

A common application for oysters is related to water treatment applications. For the absorption of phosphorus or nitrogen for example the shells can be burned and transformed into calcium oxide (CaO) (8), treated with high-pressure steam (9), turned by plasma pyrolysis into CaO (10), packed along with zeolite in columns (11) or be crushed and pyrolyzed (12). They can help decrease hydrogen sulfide concentrations (13), can replace biological aerated filters (14), capture boron from wastewaters (15), phosphate pollutants from aqueous solution (16), bind COD, BOD, NH_3 and TSS in waste water estuaries (17), copper (18) as well as cadmium (19). They can be used to synthesize calcium silicate hydrates (20), have reported good performance as contact bed purifiers (21), methylene blue capture matrixes (22), bacterial inhibitor agents in contaminated water and soil sources (23) and purification media in aquaponic systems for plant growing (24). They can also be used as functional additives in the preparation of ceramsite (25).

2.1.2 Construction applications

Another field for oyster shells is the construction sector. Crushed and dried shells have been added into concrete mixtures by improving concrete workability (26), have replaced partially the commonly used supersaturated-surface-dry sand (27) or fine sand (28) by showing good engineering properties. The shells have been calcinated and used to produce different types of bricks, with both foamed (29) or cement bricks (30) being reported. The material has also shown good potential as a foaming agent in the production of vitrocrystalline foams (31), while according to *Seo et al.* its incorporation in cement mortar improved the compressive strength (32). The surface of the material has also been modified with polyvinyl alcohol and sodium silicate and noted a positive effect on concrete mixture performance (33). In one of the most recent studies on this field, the feasibility of synthesizing cement clinkers with powdered OS (oyster shells) and scallop shells, sintered at 1470°C was evaluated, opening new opportunities for the implementation of OS (34).

2.1.3 Agriculture applications

Oyster shells are extensively used in the agriculture sector. Similar to the water treatment approach, shells are used in soils as sorbents or stabilizers. For example, the shells can be dried and crushed to improve pH and nutrient status, C and N concentrations and stimulate soil enzyme activities in soil (35) or crushed into powder and mixed with sludge to feed earthworms and produce vermicompost acting as pH soil stabilizers and enhancing worm activity (36). *Ok et al.* tested OS and calcinated-OS in their ability to stabilize heavy metals, such as Cd and Pb from heavily exploited mining showing good stabilization results with the calcinated sample performing better (37). The shells can be combusted and used as a solid catalyst to obtain 98.4wt% pure biodiesel (38), as drainage materials (39), as soil-mixing components and horizontal-drainage substrates and eventually even substitute the traditionally used sand. On a different angle, *Lee et al.* reviewed the potential use of eggshells as a soil conditioning agent and compared their recycling concept to oyster shells (40).

2.1.4 Biomedical applications

To a lesser extent, oysters have found applicability in biomedical applications. They have been used for the production of macroporous scaffolds to be seeded with pre-osteoblasts cells and to grow bone tissue in and around the scaffold with no cytotoxicity and good biocompatibility (41) or used along with dicalcium phosphate dihydrate in a planetary ball mill in order to synthesize hydroxyapatite, with the product showing good crystallinity and phase purity, important prerequisites for biomedical applications (42). Marine $CaCO_3$ from either oyster or mussel shells was tested for the preparation of alginate hydrogels to develop inorganic/organic scaffolds for bone tissue engineering (43) and have been listed as promising antioxidant peptides or else hydrolysates proteins source (44).

2.1.5 Diverse applications

The versatile nature of $CaCO_3$ can be seen in further applications. For example, calcinated and hydrated oyster shells were tested in their ability to remove SO_2 and NO_x gases from air streams showing twice the efficacy of limestone (45), crushed, calcinated and KI-impregnated OS were tested as solid catalysts (46), or showed high catalytic activity and stability in the production of a CuBr catalyst (47). Calcinated OS were found to be effective and even reusable as absorbents for anionic dyes (48), while finely crushed and dried OS were used in the synthesis of CuO and Au/CuO nanocatalyst, with the catalysts performing well and noting excellent sintering resistance (49) and the shells have also been incorporated in polypropylene based composites (50) and in CuO/ZnO nanocatalysts with higher catalyst activity compared to synthetic $CaCO_3$ (51). Because of their high Ca concentration the shells have also been fed to algae cultures showing a positive outcome by increasing the biomass yield (52) and have been also tested as a dietary calcium source for hens, confirming suitability as a Ca enrichment source without showing any negative impact on the quality (53).

3. Materials and Methods

3.1 Oyster Shells

Waste oyster shells were collected from a local restaurant (Nuremberg, Germany). They were thoroughly washed with water until all flesh remnants were removed and placed in the oven for 42 hours at 120 °C. The length of the untreated shells ranged between 6 – 10 cm. The shells were grinded by different mills and classified in fractions.

3.2 Oyster shell powder preparation- by size reduction

Before further handling, the shells were pre-crushed to a manageable size with a hammer mill, HM (LHM 20/16; Condux). To refine the hammer mill product a 5 mm sieve was placed in the ejection site. The mill had a total of 24 hammers and noted an energy consumption of 460 W, measured directly with a three-phase power analyzer (Power Quality Analyzer 434; Fluke) at a mass flow rate of 200 g/min. The crushed shells were divided into two samples, one of which was processed immediately after (unburned, uOS) while the other was burned in a muffle furnace (ASM10; Schröder Industrieöfen GmbH) for 3 hours at 550 °C (burned, bOS). This temperature was selected in order to avoid decomposition of $CaCO_3$ at temperatures above 700°C. Both samples followed the flow diagram shown in **Figure 1**.

As depicted in **Figure 1**, the oyster shells were processed with four different types of mills in total. Apart from the hammer mill, a fine impact mill (UPZ 100; Hosokawa-Alpine) was used with two of the basic interchangeable elements, the beater disc (BD) and the pin disc (PD) unit. The estimated mass flow rate was 20 g/min. The addition of a large grinding track or a small grinding track with an incorporated 0.5 mm sieve on the ejection site helped refine the product of

the BD unit even further. Lastly, the product of the BD unit (15000 rpm, large grinding track) was wet grinded by an agitated wet media mill, WM (MSM-12; Fryma Maschinen AG). For this step, three different rotation speeds were chosen, and samples were collected and analysed at different intervals of 5, 10 and 30 minutes. A 30 wt% suspension was prepared and used for the wet mill along with ball aids of 0.6 – 0.8 mm diameter as grinding media. The composition of the grinding balls was 83 % ZrO_2, stabilized with 17 % Cer(IV)-oxide (Zirkonox).

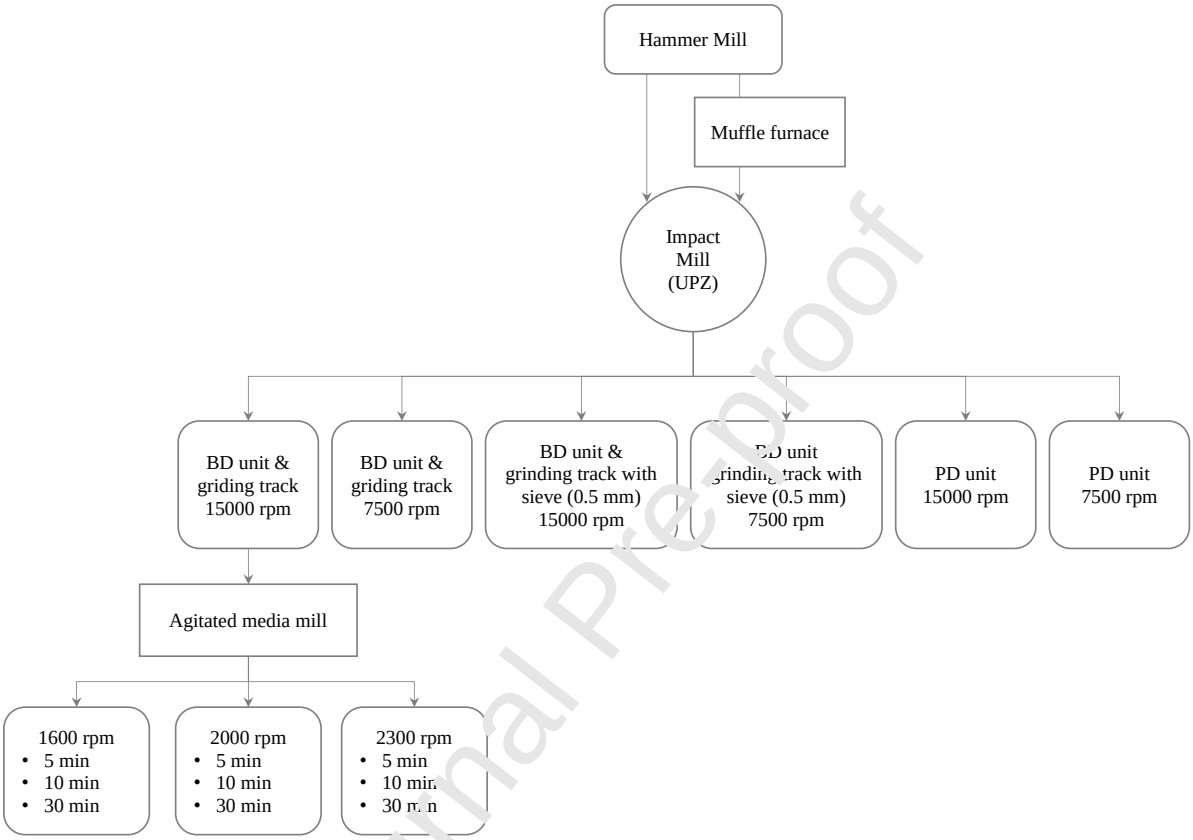

Figure 1. Flow diagram for the grinding experiments (BD stands for beater disc; PD for pin disc)

3.3 Pickering emulsion preparation

For the Pickering formulations hydrated silica, xanthan gum, glycerine, caprylic/capric triglyceride, argania spinosa kernel oil, persea gratissima (avocado) oil and tocopheryl acetate were purchased by Dragonspice Naturwaren. Citric acid was purchased from Merck and the Aerosil® R 816 particles from Evonik.

A Pickering emulsion with Aerosil® R 816 particles as stabilizers was prepared following the exact instructions as given by Evonik Industries (54). Next, the same formulation was prepared by substituting the Aerosil® R 816 particles with different concentrations of uOS particles (WM, 2000 rpm, 30 min). The Pickering emulsions stabilized by Aerosil® R 816 and uOS particles were of oil-in-water type. For concentration check purposes, the emulsions were prepared in 50 g and later in 500 g batches. The oils amounted to 23.3 % of the final volume. A further commercial product containing common surfactants, such as sodium cetearyl sulfate, ethylhexyl stearate, isopropyl palmitate and glyceryl stearate was purchased and used in the stability comparison section constituting the three different samples or formulations tested in this study.

For the uOS Pickering formulation the components of the oil phase were initially mixed together (500 rpm, 5 minutes) using an overhead stirrer with a propeller mixer (RW 20 digital;

IKA) while the uOS particles were in parallel added to the water phase and dispersed by a high-performance disperser (T25 digital Ultra-Turrax; IKA) at 13000 rpm for 15 min. Later on, the two phases were slowly combined and mixed further for 10 – 15 min and their pH was duly adjusted to 6 – 6.5 by adding 10 wt% citric acid solution. The pH was adjusted in order to keep the dissolution rate or $CaCO_3$ to a minimum and make the product appropriate for a skin application.

Ultimately, the emulsions were stored for the experimental period in airtight containers at 25 °C. The formulations were analysed over a period of 8 weeks by means of an analytical centrifuge and their size distributions estimated by laser diffraction.

3.4 Analytical methods

The different grinded fractions were analysed by laser diffraction spectroscopy (Helos KR; Sympatec) after first sieving the products and collecting the finest fraction <32 μm. The shape was observed under light microscopy (Axiotech 105 color; Zeiss) and the morphology by a scanning electron microscopy (SU8000; Hitachi High-Tech). The SEM images were acquired at an accelerating voltage of 1 kV. The specific surface area was measured with the Brunauer-Emmett-Tellet Method (BET; Nova 2000e, Quantachrome) and a 5 Point estimation between 0.05 and 0.35 (P/P_0). The sample degassing took place for 17 hours at 130 °C. Contact angles for the powders were estimated by a tensiometer according to the Washburn method (K100; Krüss) by using nonane, lemongrass oil, eucalyptus oil and diiodomethane all purchased from Karl Roth.

The stability of the Pickering formulations was further analysed by an analytical centrifuge (LumiSizer; LUM GmbH), a light microscope (Axiotech 105 color; Zeiss) and a rheometer (Physica UDS 200, Measuring system MP 30, Measuring cell TEK 180; Anton Paar), while the droplet distributions were estimated by the Helos KR; Sympatec.

4. Results and Discussion

4.1 Pretreatment and characterization of oyster shells powder

Oyster shells were treated with four mills as was shown in **Figure 1**. To observe the morphology and shape of the particles the grinded product was sieved and the finest fraction (< 32 μm) of each mill was observed by a scanning electron microscope (**Figure 2)**.

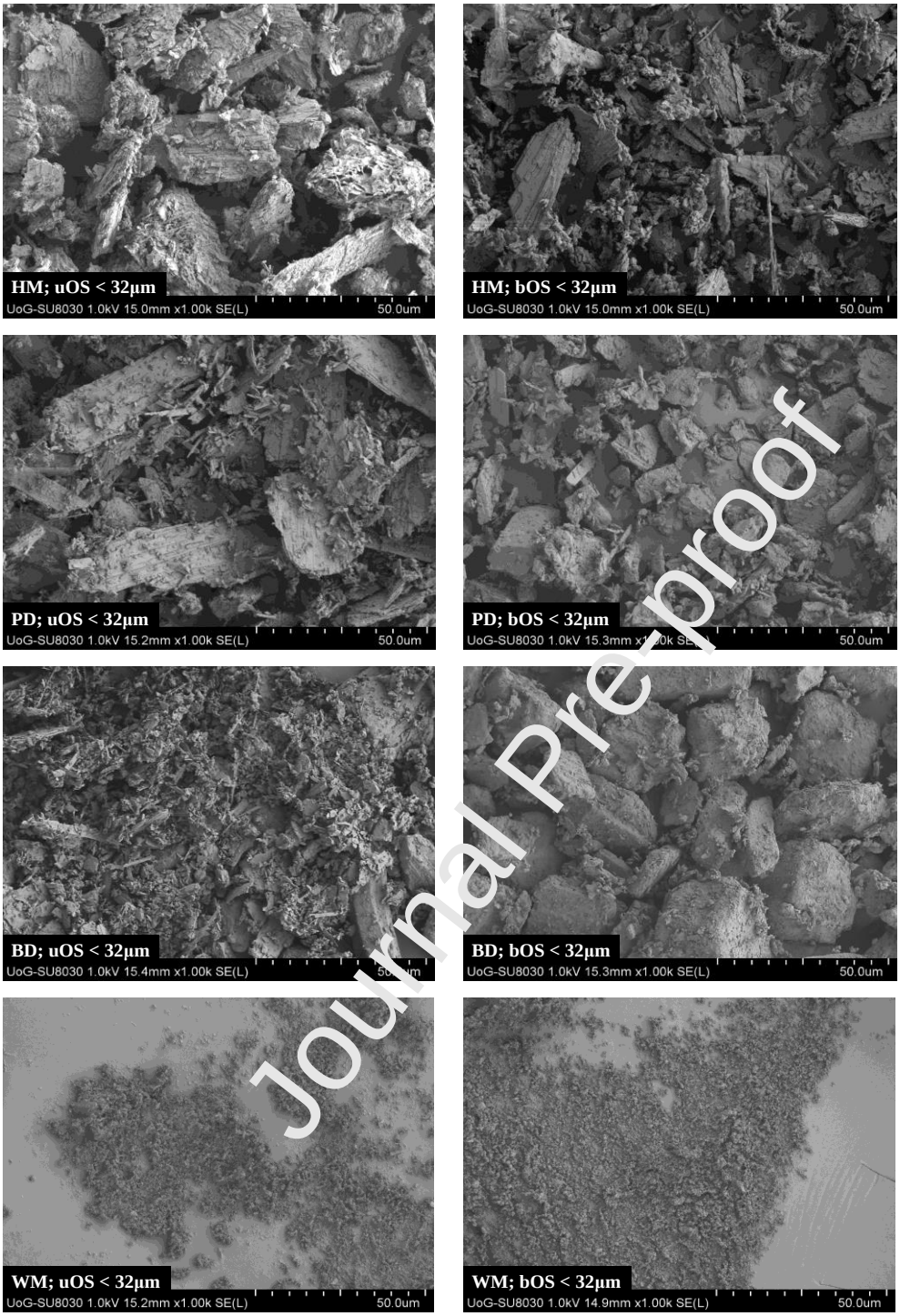

Figure 2. SEM captures of the finest sieved fraction < 32 µm of unburned oyster shells (uOS) and burned oyster shells (bOS) obtained after treatment by the hammer mill (HM), pin disc mill (PD), beater disc mill (BD) and agitated wet media mill (WM). Scale bar is set at 50 µm

The particles obtained by the HM appear to have a platelet like form with a lot of fractured finer residue. In the uOS the different layers of the shells are also visible, which is less so in the bOS. The difference between the two samples is more noticeable when comparing PD and BD. Starting with the PD, the uOS can be easily identified in a platelet like form with a pronounced share of needle shaped particles, while the bOS appears to have turned into a compacter square-like

shaped form. This effect is even more evident in the BD obtained fraction, with the uOS being fractured further down into needle shaped particles and the bOS showing a rounder form with less percentage of fines. No variation is apparent when observing the resulted particles of the wet mill (WM). However, the particles processed by the WM have a considerable smaller size, appear more homogeneous, narrower distributed and show fewer sharp edges in comparison to the rest of the mills tested. The specific surface area and the particle size of the finer fraction obtained by the PD, BD and WM are given in **Table 1**.

Table 1. Specific surface area (SSA) obtained by a 5 Point BET analysis and media values estimated by laser diffraction analysis for uOS and bOS from processing the oyster shells in the pin disc mill, beater disc mill and agitated wet media mill. The standard deviation given in SSA is the maximum observed in the samples.

Mill type	**Speed [rpm]**	**Time [min]**	**SSA [m²/g] uOS** ±0.08	**x_{50} [µm] uOS**	**SSA [m²/g] bOS** ±0.08	**x_{50} [µm] bOS**
PD	15000	-	2.70	31.23	1.27	11.27
	7500	-	1.71	178.68	0.85	45
BD	15000	-	5.15	3.62	1.64	5.1
	7500	-	4.32	16.52	1.37	14.1
BD with 0.5 mm sieve	15000	-	4.26	5.55	1.53	7.34
	7500	-	3.29	24.54	1.36	24.96
WM	1660	5	11.81	1.69	5.50	1.85
	1660	10	13.03	1.33	6.56	1.49
	1660	30	14.05	0.83	9.13	0.88
	2000	5	11.28	1.77	6.72	1.64
	2000	10	12.16	1.43	7.66	1.28
	2000	**30**	**17.16**	**0.79**	8.75	0.78
	2310	5	10.60	2.31	5.13	1.80
	2310	10	12.17	1.76	6.43	1.49
	2310	30	14.51	1.00	9.55	0.82

As shown in **Table 1**, the specific surface area of the uOS was in all cases higher than the bOS. We attribute this effect to the 3 hours muffle furnace heating process at 550 °C that eliminated part of the organic matter decreasing the surface area due to agglomeration and incipient sintering. What can also be seen in **Figure 2** is a transformation of the particles' surface from a rough to a smooth texture which further explains the drop of the SSA as it removes asperities.

The change in particle shape is also reflected through the particle size analysis. The shift, in some cases, from a needle-shape to a square-shape with round edges observed in Figure 2 is echoed in the results. The PD milling appears to have resulted in finer particles for the bOS. The 15,000 rpm milling of uOS exhibited an x_{50}=31.23 µm while the bOS noted x_{50}=11.27 µm. This comes in agreement with the SEM observations, if one considers that even the uOS finer sieved fraction shows larger particles than its analogous bOS. However, observations differ for the BD mill, where again the SEM captures support the x_{50} findings of **Table 1**. The BD sample without the incorporated sieve shown for uOS in **Figure 2** appears to be finer than the bOS. The same applies for the WM measured fractions, which appear to have less variations for uOS and bOS.

To characterize the surface free energy of burned and unburned oyster shells, we measured contact angles with force tensiometry according to the Washburn method and estimated the polarity of the surface (55). The method relies on the capillary rise of a fluid in a powder bed

when a contact between the two is established. The weight of the liquid is recorded with respect to time and used to estimate a contact angle that demonstrates the wettability of the sample. For this set of experiments, we used the burned and unburned fraction from the agitated wet media mill at 2000 rpm after 30 min that were later used in the Pickering emulsions.

Figure 3 shows the contact angle results obtained from wetting the powders using nonane, lemongrass, eucalyptus oil, sunflower oil, diiodomethane and water (from left to right). In order to increase the accuracy of the Washburn method it is important to choose test fluids that have different surface tensions and polarity. The contact angles shown in **Figure 3** were used to estimate the surface free energy of oyster shells according to the OWRK model. For the uOS the surface free energy (SFE) was calculated as 32.53 mN/m with a polar part of 11.28 mN/m. The bOS sample showed a surface free energy at 25.33 mN/m and a polar part of 8.33 mN/m.

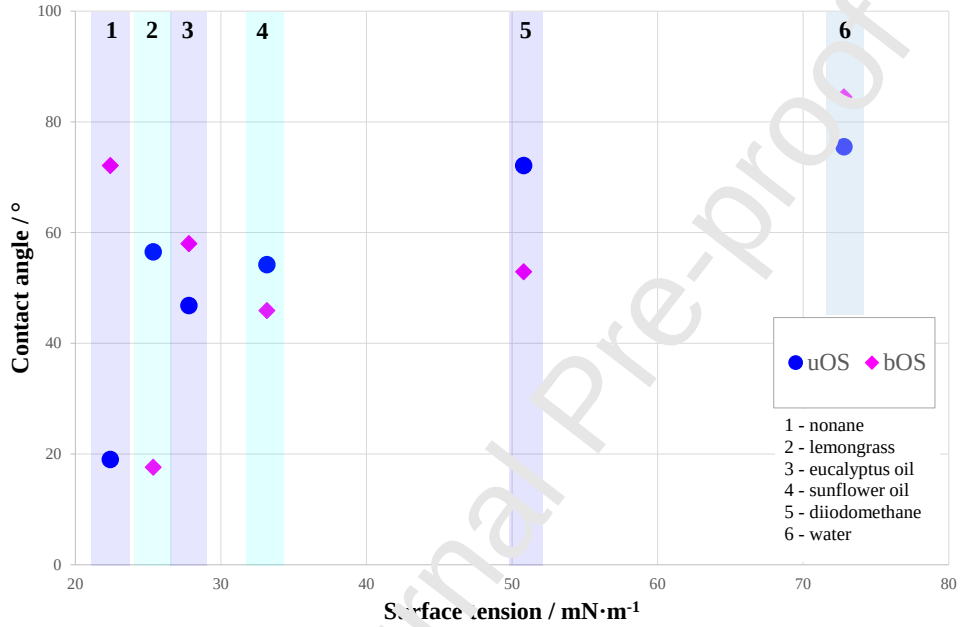

Figure 3. Contact angle measurements with different liquids for uOS and bOS

Based on the characterization results we decided to process in the Pickering emulsions the unburned fraction obtained by the agitated wet media mill at 2000 rpm after 30 min. This fraction showed both the finest media at x_{50}=0.79 μm the highest SSA at 17.16 m^2/g, the highest SFE at 32.53 mN/m and at the same time the particles were perceived to be quasi-spherical. Another reason to justify why the uOS was preferred is because the contact angle measured when immersed in water is slightly lower (75.5° for uOS and 84.5° for bOS), which translates into a better immersion of the particles in the water phase. A higher contact angle means that the particles are less adequately immersed in water. A smaller contact angle represents a higher spreading of the fluid on the surface and a better wettability. From the two contact angles estimated above, the bOS is more hydrophobic than the uOS sample. Complimenting the above statement, literature references have stated a higher stability of emulsions with intermediate hydrophobicity particles while very hydrophilic or hydrophobic particles caused the system to separate (56).

Pickering emulsions are more stable if the particles can position themselves on the oil – water interface, since a complete immersion in one of the phases could quickly result in a suspension of particles without creating a boundary layer. Alongside the higher affinity to water the sample

showed a higher SFE which means better wettability. Unburned OS showed a higher contact angle with diiodomethane which is considered to be a non-polar liquid, but the opposite occurred with nonane, which again as an alkane in considered to be non-polar. One could argue that the longer chain of nonane and the resulting dipole moment is sufficient to explain the outcome. However, the higher SFE and contact angle to water helped in choosing the uOS. In terms of wetting, as it is a comparison method and requires a liquid assumed to completely wet the surface, rapeseed oil (33.03 mN/m) was measured and showed complete wetting for uOS while for bOS this was noted with soybean oil (31.45 mN/m).

4.2 Pickering emulsions

Pickering emulsions with Aerosil® R 816 and uOS particles were prepared. In order to test the uOS particles in the system a concentration check was followed according to the procedure described in the section below.

4.2.1 Concentration check

In the test phase of the development process, 50 g Pickering emulsions with 2, 4, 6, 8 and 10 wt% uOS concentration were prepared. The droplet size distribution of the five different formulations are shown **Figure 4**. The cuvettes after a centrifugation cycle including a control one without any particles (0 wt%) are also reported in figures 4a and 4b.

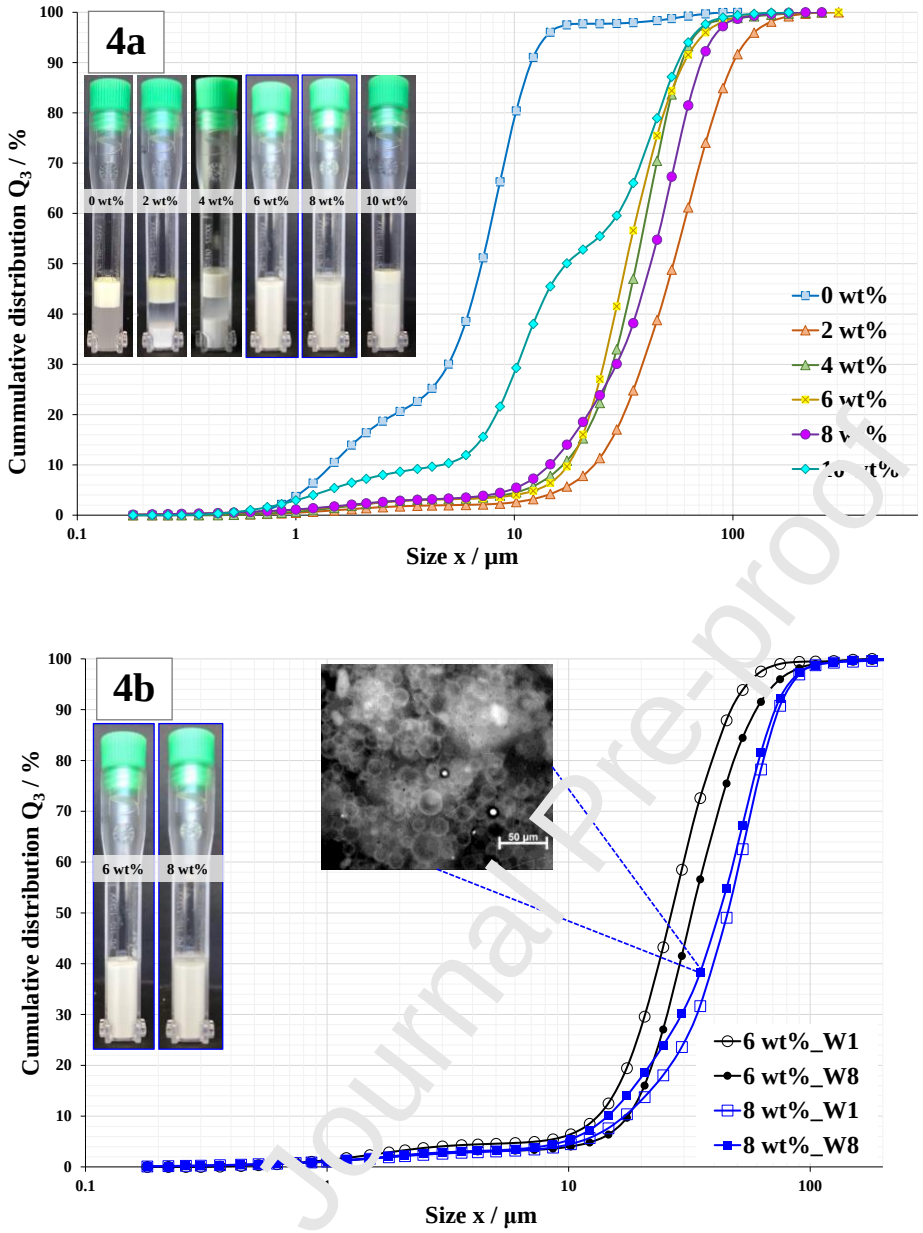

Figure 4. Cumulative droplet size distribution for the control sample and the samples containing 2, 4, 6, 8 and 10 wt% uOS (4.a) and distributions measured by week 1 and week 8 for the samples containing 6 wt% and 8 wt% uOS with a light microscope capture of the formed droplets for week 8, 8 wt% (4.b). The cuvettes show the separation tendency of the samples after an analytical centrifuge cycle at 4000 rpm for 83 min

Figure 4.a gives the droplet size distribution of the uOS samples. The control formulation containing no particles was measured once immediately after preparation to demonstrate the oil droplet size, measured at 6.8 ±0.4 µm. The oil droplets however, are not stabilized and the formula separates into two phases in a matter of few hours. The rest of the samples were measured in triplicates weekly for a total period of 8 weeks.

The 2 wt% sample showed an initial x_{50}=87.24 μm that slowly decreased over the weeks reaching a value of 53.44 μm by week 8. The insufficient number of uOS particles was unable to cover the dispersed oil droplets and resulted in desorption from the oil droplets over time that increased the proportion of fines in the sample.

The 4 wt% formulation showed no changes in the eight weeks and the media was estimated at 35.6 ±0.3 μm. This was different for the 6 wt% where an initial media of 26.72 μm with an increasing tendency reached 32.55 μm by week 8. The formulation did not show any optical alterations during this time nor any phase separation. The 8 wt% samples had a starting media of 45.5 μm and showed a decrease by week 8 at 42.2 μm. The final sample, at a 10 wt% concentration had an initial x_{50}=14.74 μm that changed to x_{50}=18.29 μm.

To further depict the separation resistance, the samples were subjected to a centrifuge cycle at 4000 rpm for 83 min. The cuvettes after the centrifuge cycle are shown in **Figure 4.a**. As is clearly visible, a limited number of particles is unable to stabilize the oil phase in the water and the particles sediment after centrifugation to the bottom, as in the case of the 2 wt%, formulation. A layer of oil droplets covered with particles is fairly visible above the particles, with however the majority of the oil fraction migrating to the surface. By increasing the concentration to 4 wt%, the emulsion forms three distinct layers. On the top there is an oil phase with a small percentage of trapped particles, moving downwards a water layer and finally a bottom layer where the particles have sedimented. By further increasing the concentration, both the 6 and 8 wt% formulated samples efficiently transition to a more homogeneous system.

In the case of the 8 wt% concentration a top layer of water appears to have formed on the surface. We postulate that this can result from the fact that the oil phase is finely dispersed and covered by particles having thus a higher density and forming a compact layer at the bottom. This result is promising in terms of long-term stability, as it is often established when the disperse phase is evenly and finely distributed in the continuous phase. Finally, by increasing yet again the concentration, the maximal coverage of the oil phase is exceeded, and the particles appear to agglomerate and form a layer at the bottom, while an oily phase is now again visible in the surface of the particulate sample.

A demonstration of the shift seen in the 6 wt% and 8 wt% sample is depicted for week 1 and week 8 in **Figure 4.b**. If the boundary of the oil droplets is not substantially covered by particles, the oil droplets can flocculate, coalesce and cause slow or immediate phase separation. A stable size of the droplets signifies adequate coverage by particles and minimal system changes over time. Based on the results for the two samples the 8 wt% formulation was subjected to further stability tests by incorporating rheological analysis.

4.3 Oysters, Aerosil and Surfactants

The uOS formulation (8 wt%) was subjected along with the original Evonik formulation (2 wt% Aerosil R816) and a store-bought product to further testing. To the naked eye, the uOS formulation had a slightly greyish colour in contrast to the other two. In terms of texture, the uOS had a lotion consistency while the other two resembled a cream. The three formulations were analysed for a period of 8 weeks. **Figure 5**, shows the droplet distribution featured using light microscopy.

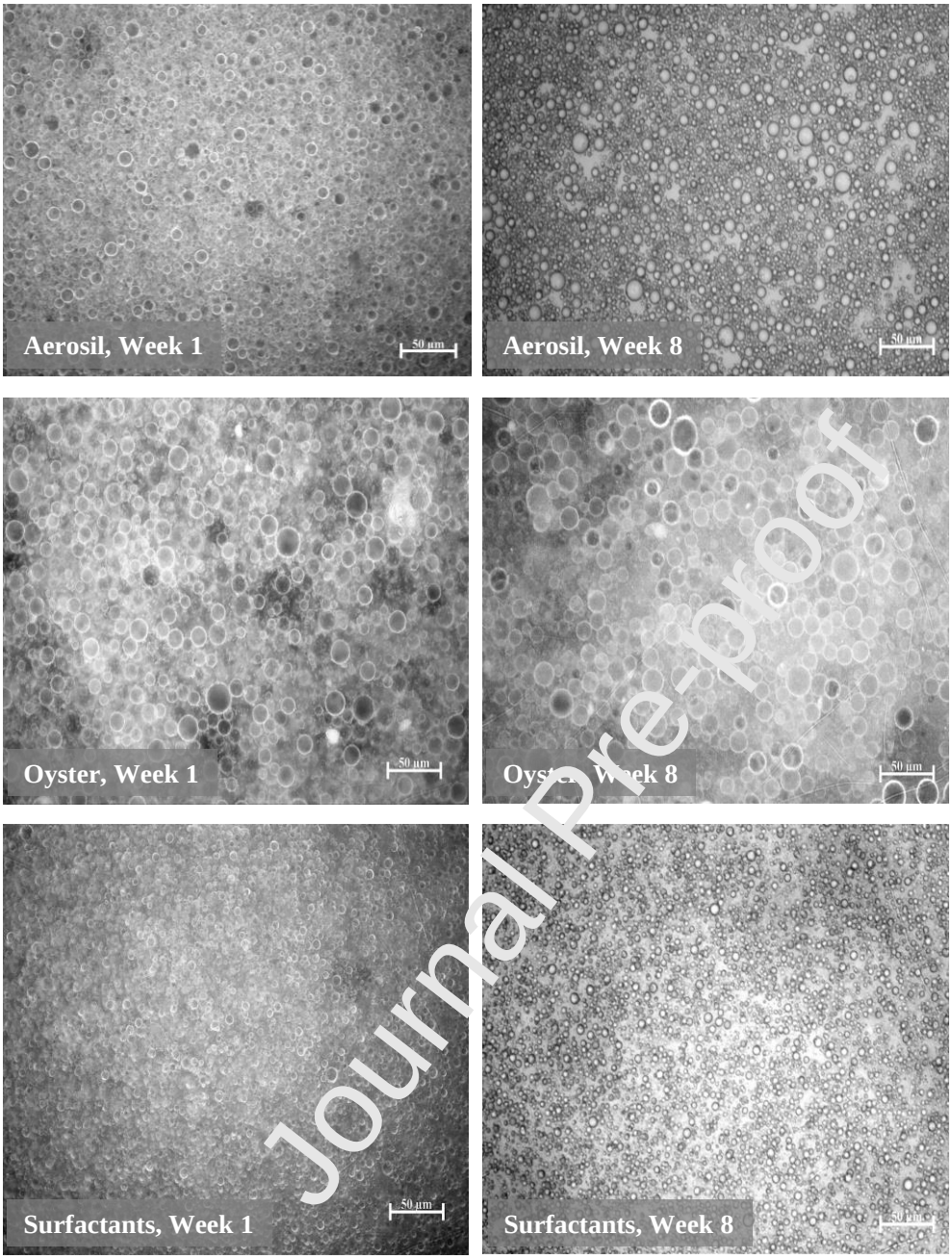

Figure 5. Light microscopy captures for the samples containing Aerosil particles, uOS and surfactants at week 1 and week 8, 200× magnification, scale bar at 50 µm

The captures shown in **Figure 5**, depict the droplets of the formulation. The Aerosil containing formulation, has a proportion of large droplets around 10 µm with the majority of them being smaller than that. The uOS formulation, shows the largest droplets of the three samples at about 20 µm, while the surfactant emulsion has the smallest droplets at presumably below 5 µm. In terms of change in the systems in the course of 8 weeks, the Aerosil formulation appears to have an increase in the proportion of large droplets. To further support this, droplet distributions are given in **Figure 6**.

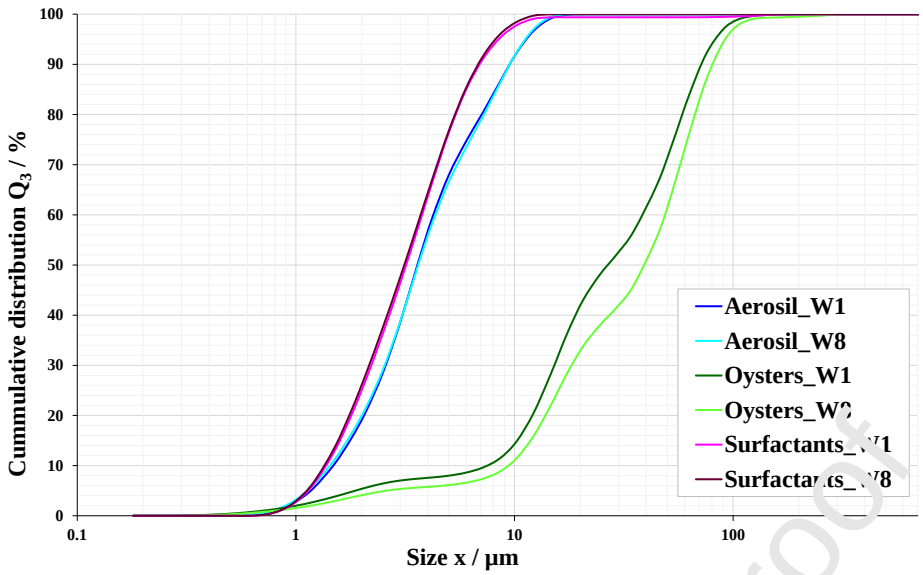

Figure 6. Cumulative droplet size distributions estimated at week 1 and week 8 for the three formulations.

The distributions shown in **Figure 6** correlated well with the microscopy observations. The results showed no changes for the Aerosil formulation exhibiting a x_{50}=3.6 µm, nor for the surfactant sample with an x_{50}=3.2 µm. The EOS sample showed a change as the weeks passed by with the media shifting from x_{50}=26.8 µm to x_{50}=39.2 µm. This does not correlate with the visual inspection of the sample as seen under the microscope.

In terms of structure composition, this is better reflected by rheological measurements and to corroborate that, the samples were measured weekly in triplicates by means of rotation and oscillation measurements. In order to affect the least possible the structure of the emulsions, a sample was carefully placed on the measuring plate of the rheometer and was left to relax for 2 minutes prior to each measure. Additionally, it is important to mention here that for the duration of 8 weeks the samples were not mixed nor shaken and were gathered for the measurements with the least agitation possible. The dynamic viscosity is given in **Figure 7** for the different samples at week 1 and 8. In order to compare the change in viscosity over the test period, a measuring point found in the rising range of the viscosity curves at shear rate 8.91 s^{-1} was selected and the mean values of the dynamic viscosity were plotted against the time in Figure 7 (bottom).

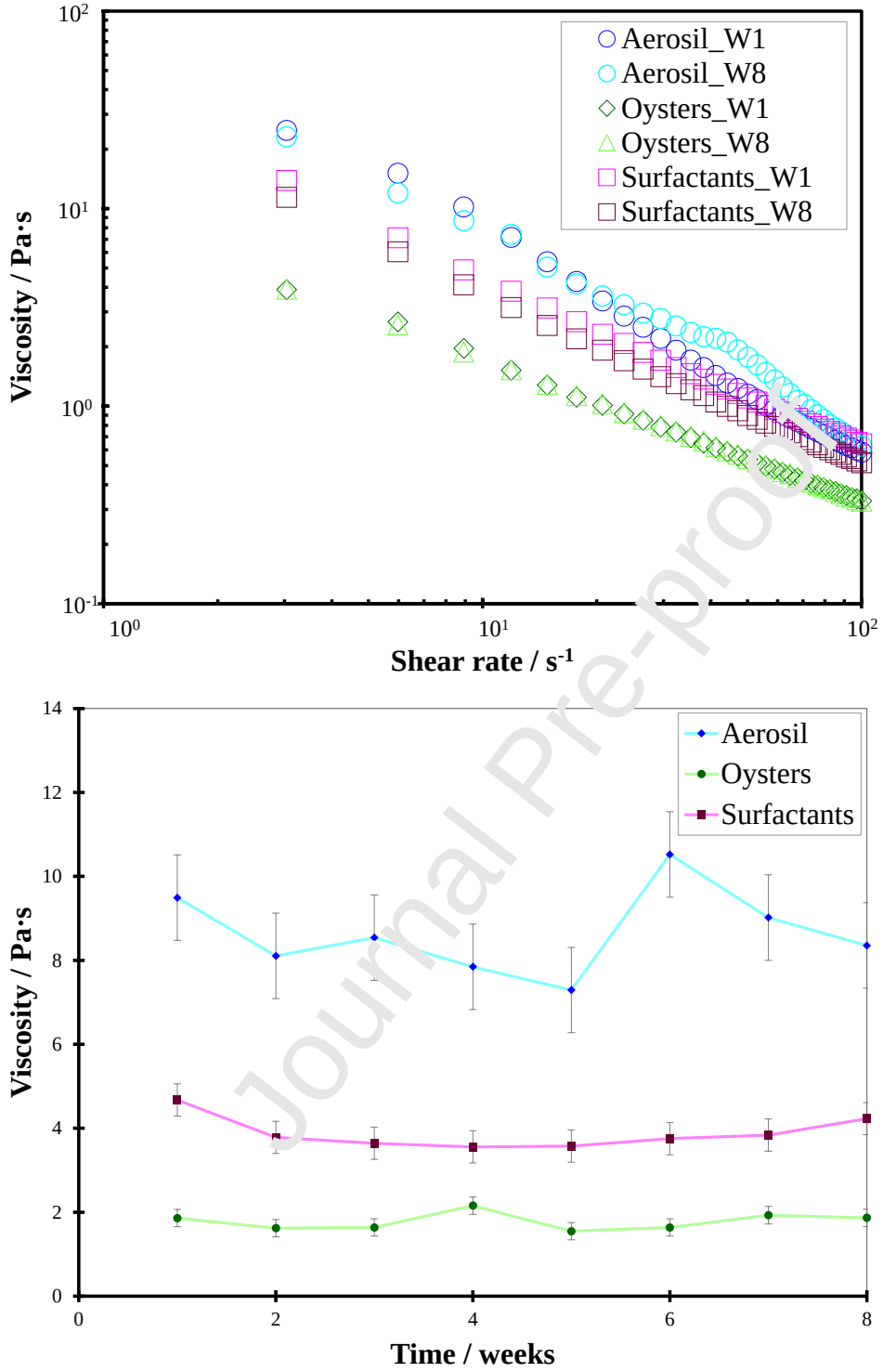

Figure 7. Viscosity curves for the three samples (Aerosil, Oyster and Surfactants) measured at week 1 and week 8 and dynamic viscosity at a shear rate of 8.91 s^{-1} plotted against a period of eight weeks

From the viscosity curves given in **Figure 7**, it can be concluded that in the given amount of time the dynamic viscosity remained unchanged.

All samples show a viscosity decrease with increasing shear rate, which is typical for shear thinning liquids. This is to be expected with emulsions as deformation of the finely distributed oil droplets from spheres to ellipsoids occurs with increasing shear rate and thus the internal friction decreases. The fact that the dynamic viscosity does not change much over time indicates that the structure of the emulsions forms quickly, and the oil droplets remain stable.

Apart from the rotational tests, amplitude sweep tests were carried out for each formulation. By an amplitude sweep, which is an oscillatory test, information about the mechanical stability, the structure strength and the viscoelastic character of an emulsion can be collected. The test measures the storage modulus G', which shows the energy stored in the sample and translates to its elastic response while the loss modulus G" measures the energy losses in the sample and gives the sample's viscous character. The graphs in Figure 8 are shown in a double logarithmic plot of the storage modulus (G') and loss modulus (G") as a function of oscillation shear stress for a) aerosil, b) oysters and c) surfactants.

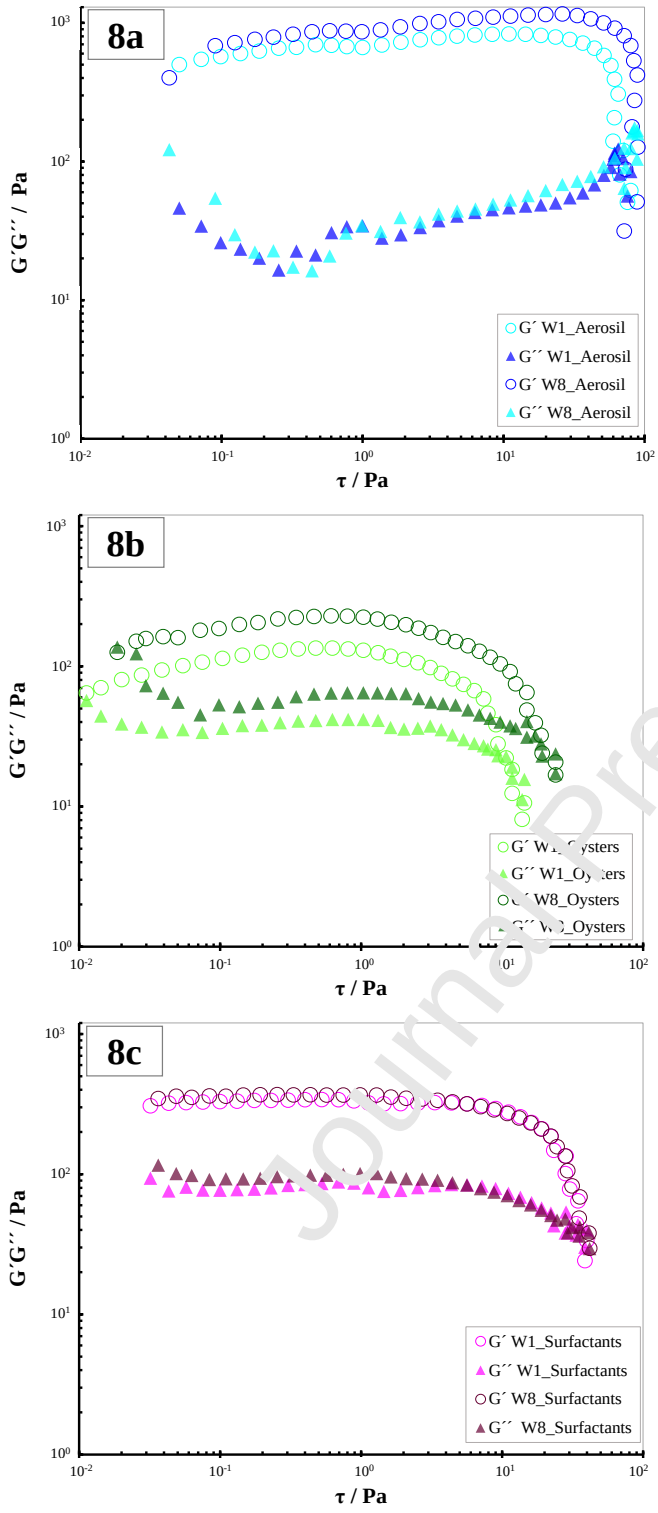

Figure 8. Amplitude sweeps for the different samples at week 1 and 8. a) aerosil, b) oysters and c) surfactants. Experiment was conducted in triplicate.

In the amplitude sweep G' is above G" which means that in this range the viscoelastic character of the sample prevails up to their intersection where the structure is irreversibly impaired. It is

striking that G' is relatively linear while G" shows strong deviations from a linear course. This behaviour is particularly noticeable in both Pickering emulsions (Aerosil and Oyster) and could be caused by the pre-shearing of the sample by applying it with a spoon spatula. From the plots shown in **Figure 8**, the yield point τ_γ, flow point τ_f and the linear-viscoelastic range LVE can be evaluated graphically. The τ_γ in this case is the lowest shear-stress value above which the liquid character of the sample prevails while the LVE range lies before the τ_γ. In the LVE range, any deformation caused by shearing is so small that the structure remains intact. The flow point, τ_f is found at the intersection of G' to G". After the intersection point, G"> G', so the liquid character of the sample predominates. A further indication that can be inferred from **Figure 8** is the firmness of the sample. The larger the distance between G' to G" the firmer the sample is. This is the case for the Aerosil sample. Another indication that can be assumed here, is a higher value noted for the crossover as well as a τ_f value indicating a more stable sample.

The estimated values of τ_γ, τ_f as well as the LVE range for the samples are shown for week 1 and 8 in **Table 2**.

Table 2. Yield point $\boldsymbol{\tau_\gamma}$, the flow point $\boldsymbol{\tau_f}$ and LVE range for week 1 and 8

	Aerosil		**Oysters**		**Surfactants**	
Value	**Week 1**	**Week 8**	**Week 1**	**Week 8**	**Week 1**	**Week 8**
$\boldsymbol{\tau_\gamma}$ **/ Pa**	29.50 ±1.4	29.17 ±1.2	1.62 ±0.3	1.75 ±0.5	11.10 ±0.4	10.57 ±0.2
$\boldsymbol{\tau_f}$ **/ Pa**	61.20 ±1.6	61.20 ±1.4	10.70 ±0.2	15.73 ±0.9	30.20 ±0.8	34.97 ±0.8
LVE / Pa	0.05 - 4.67	0.05 - 5.23	0.01 - 1.32	0.02 - 1.39	0.03 - 9.01	0.03 - 8.58

The results of **Table 2** show no significant change during the 8-week test period. This means that the structure of the emulsions forms quickly and remains stable for a longer period of time. Three weeks after the study period (week 11) the samples were subjected to a frequency sweep in order to generate information about their time-dependent behaviour. The frequency sweep was conducted at a frequency range of 100 to 0.1 s^{-1} (**Figure 9**).

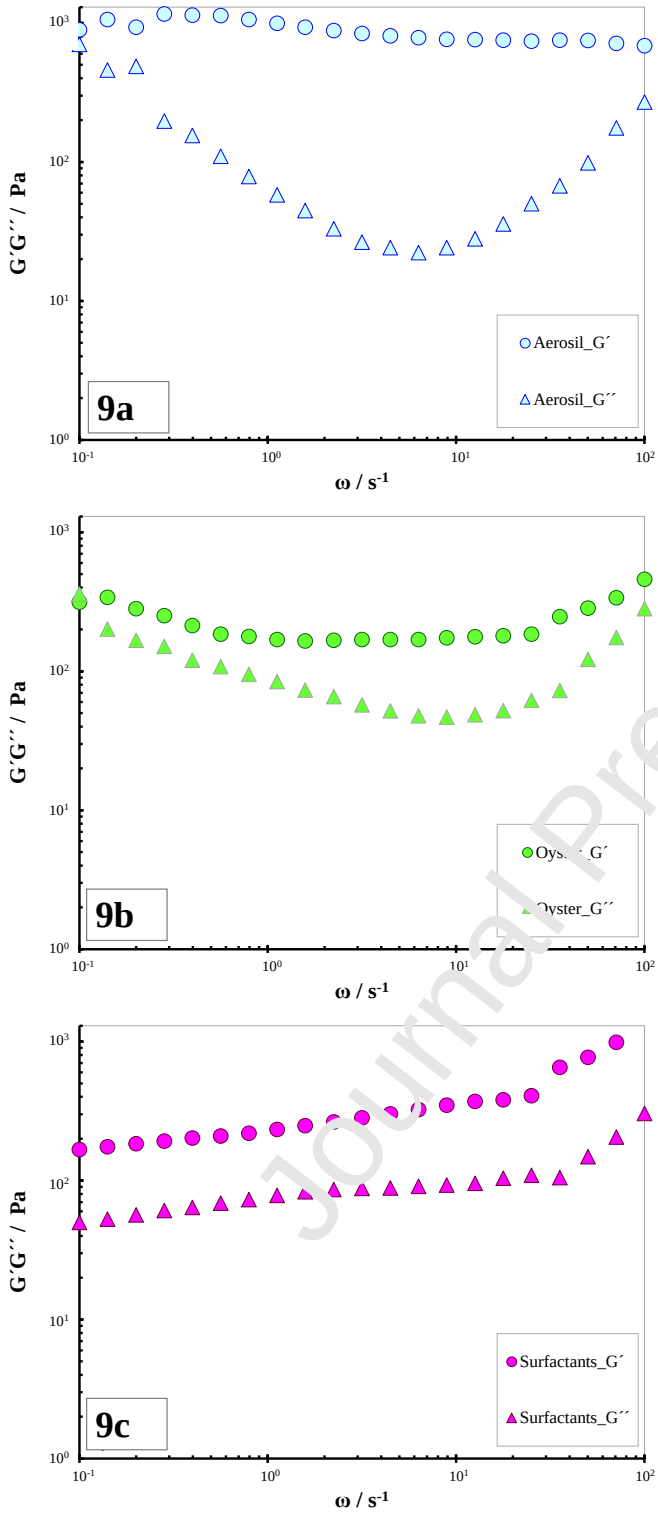

Figure 9. Frequency sweeps for the different samples at week 11. a) aerosil, b) oysters and c) surfactants. Experiment was conducted in triplicate.

In frequency sweeps, low frequencies are used to simulate slow motions and high frequencies fast ones. A parallel course of G' to G" reflects stability both at rest and agitation. For both Pickering emulsions a tendency for phase separation is observed as G' and G" intersect or strongly converge

towards the end, with no readable indication when this could take place. This is different for the surfactant sample, where G' and G" show no intersection, meaning that the emulsion is stable against sedimentation and creaming. For all three formulations the viscoelastic character prevails as G' progresses above G". At the same time, the short-term behaviour of the samples in the middle to high frequency range shows a parallel course and can be interpreted as structure stability in this range. Additionally, measuring fluctuations noted for G" can be caused by an insufficient pause of 3 min prior to measure intended to allow the internal structure to form at rest. The same can be said for the measuring point duration which can be also increased.

5. Conclusions

Oyster shells are a valuable material that can be used in a number of ways. As a natural material, a crucial step in the reutilization process comes from the initial treatment, well understood material properties and an overall energetically viable preparation. We prepared in total eight fractions of burned and unburned oyster shells by different mills. From them, the oyster shells that were treated first with a hammer mill, then a beater disc mill and finally a wet media mill for 30 min were used for the preparation of the emulsions.

What further influenced our decision to proceed with this fraction was the wettability results. Ideally in Pickering emulsions the particles have to position themselves in between the two liquids and form a stable boundary layer. It is difficult to draw exact conclusions about the inclination of the particles to each fluid, especially as both phases in cosmetic formulations are mixtures but a distinction between two materials can still be made.

For the particle stabilized emulsions, the use of a high concentration of oysters (8 wt%) is viewed as a good outcome, since a substantial amount could find repurposing this way. In terms of stability, the oyster shell formulation showed a relative stable character despite a slight tendency towards separation compared to the other commercial formulations. By further tuning the formulation this initial stability could be enhanced. Oyster shells showed no significant alterations in the droplet distributions nor irreversible formation of agglomerates for the tested period.

We have demonstrated no significant viscosity alterations in the samples studied. The yield point and flow point, important for transport and application of the emulsions, remained relatively stable. The same was observed for the LVE range. The results of the frequency tests showed a steady short-term behaviour while for the long-term behaviour, only the surfactant sample could be categorised with confidence as stable. Based on our results, we expect promising applicability of oyster shells as particle stabilisers in complex emulsion formulations of cosmetics or other type of systems, such as paints.

Acknowledgments

The helpful comments of Roland Gross from the TH Nürnberg Georg Simon Ohm are acknowledged with thanks. The reviewers are acknowledged for very helpful and insightful comments on the first manuscript.

CRediT author statement

Makrina A Chairopoulou: Conceptualization, Methodology, Investigation, Formal Analysis, Writing- Original draft preparation & Editing.

Pablo Garcia-Triñanes: Conceptualization, Methodology, Formal Analysis, Writing- Original draft preparation, Writing - Review & Editing, Resources

Ulrich Teipel: Project administration, Supervision, Funding acquisition, Writing - Review & Editing

Declaration of interests

The authors declare that they have no known competing financial interests or personal relationships that could have appeared to influence the work reported in this paper.

The authors declare the following financial interests/personal relationships which may be considered as potential competing interests

References

1. Etheridge, S. M. Paralytic shellfish poisoning: seafood safety and human health perspectives. *Toxicon : official journal of the International Society on Toxinology [Online]* **2010,** *56* (2), 108–122.
2. FAO. Fishery and Aquaculture statistics 2017 [Online] **2017**.
3. FAO. Species Fact Sheets: Crassostrea virginica [Online] **2007**.
4. Yoon, G.-L.; Kim, B.-T.; Kim, B.-O.; Han, S.-H. Chemical–mechanical characteristics of crushed oyster-shell. *Waste Management [Online]* **2003,** *23* (9), 825–834.
5. Lee, S.-W.; Jang, Y.-N.; Ryu, K.-W.; Chae, S.-C.; Lee, Y.-H.; Jeon, C.-W. Mechanical characteristics and morphological effect of complex crossed structure in biomaterials: fracture mechanics and microstructure of chalky layer in oyster shell. *Micron (Oxford, England : 1993) [Online]* **2011,** *42* (1), 60–70.
6. Yang, Y.; Fang, Z.; Chen, X.; Zhang, W.; Xie, Y.; Chen, Y.; Liu, Z.; Yuan, W. An Overview of Pickering Emulsions: Solid-Particle Materials, Classification, Morphology, and Applications. *Frontiers in pharmacology [Online]* **2017,** *8*, 287.
7. Huang, F.; Liang, Y.; He, Y. On the Pickering emulsions stabilized by calcium carbonate particles with various morphologies. *Colloids and Surfaces A: Physicochemical and Engineering Aspects [Online]* **2019,** *580*, 123722.
8. Kwon, H.-B.; Lee, C.-W.; Jun, B.-S.; Yun, J.; Weon, S.-Y.; Koopman, B. Recycling waste oyster shells for eutrophication control. *Resources, Conservation and Recycling [Online]* **2004,** *41* (1), 75–82.
9. Namasivayam, C.; Sakoda, A.; Suzuki, M. Removal of phosphate by adsorption onto oyster shell powder?kinetic studies. *J. Chem. Technol. Biotechnol. [Online]* **2005,** *80* (3), 356–358.
10. Jae Ou Chae; S. P. Knak; A. N. Knak; H. J. Koo; V. Ravi. Oyster shell recycling and bone waste treatment using plasma pyrolysis. *Plasma Science & Technology [Online]* **2006,** *8* (6), 712 - 715.

11. Jung, Y.-J.; Koh, H.-W.; Shin, W.-T.; Sung, N.-C. A novel approach to an advanced tertiary wastewater treatment: Combination of a membrane bioreactor and an oyster-zeolite column. *Desalination [Online]* **2006,** *190*, 243–255.

12. Lee, C. W.; Kwon, H. B.; Jeon, H. P.; Koopman, B. A new recycling material for removing phosphorus from water. *Journal of Cleaner Production [Online]* **2009,** *17* (7), 683–687.

13. Asaoka, S.; Yamamoto, T.; Kondo, S.; Hayakawa, S. Removal of hydrogen sulfide using crushed oyster shell from pore water to remediate organically enriched coastal marine sediments. *Bioresource technology [Online]* **2009,** *100* (18), 4127–4132.

14. Liu, Y.-X.; Yang, T. O.; Yuan, D.-X.; Wu, X.-Y. Study of municipal wastewater treatment with oyster shell as biological aerated filter medium. *Desalination [Online]* **2010,** *254* (1-3), 149–153.

15. Tsai, H.-C.; Lo, S.-L.; Kuo, J. Using pretreated waste oyster and clam shells and microwave hydrothermal treatment to recover boron from concentrated wastewater. *Bioresource technology [Online]* **2011,** *102* (17), 7802–7806.

16. Chen, W.-T.; Lin, C.-W.; Shih, P.-K.; Chang, W.-L. Adsorption of phosphate into waste oyster shell: thermodynamic parameters and reaction kinetics. *Desalination and Water Treatment [Online]* **2012,** *47* (1-3), 86–95.

17. Luo, H.; Huang, G.; Fu, X.; Liu, X.; Zheng, D.; Peng, J.; Zheng, K.; Huang, B.; Fan, L.; Chen, F.; Sun, X. Waste oyster shell as a kind of active filler to treat the combined wastewater at an estuary. *Journal of Environmental Sciences [Online]* **2013,** *25* (10), 2047–2055.

18. Wu, Q.; Chen, J.; Clark, M.; Yu, Y. Adsorption of copper to different biogenic oyster shell structures. *Applied Surface Science [Online]* **2014,** *311*, 264–272.

19. Alidoust, D.; Kawahigashi, M.; Yoshizawa, S.; Sumida, H.; Watanabe, M. Mechanism of cadmium biosorption from aqueous solutions using calcined oyster shells. *Journal of environmental management [Online]* **2015,** *150*, 103–110.

20. You, W.; Hong, M.; Zhang, H.; Wu, Q.; Zhuang, Z.; Yu, Y. Functionalized calcium silicate nanofibers with hierarchical structure derived from oyster shells and their application in heavy metal ions removal. *Physical chemistry chemical physics : PCCP [Online]* **2016,** *18* (23), 15564–15573.

21. Shih, P.-K.; Chang, W. L. The effect of water purification by oyster shell contact bed. *Ecological Engineering [Online]* **2015,** *77*, 382–390.

22. Jung, S.; Heo, N. S.; Kim, E. J.; Oh, S. Y.; Lee, H. U.; Kim, I. T.; Hur, J.; Lee, G.-W.; Lee, Y.-C.; Huh, Y. S. Feasibility test of waste oyster shell powder for water treatment. *Process Safety and Environmental Protection [Online]* **2016,** *102*, 129–139.

23. Shin, Y. B. Bio-Controlling Effect of Oyster Shell on Bacteria in Polluted Soil and Water in Seaside Areas. *APEC Youth Scientist Journal [Online]* **2016,** *8*, 219–230.

24. Yen, H. Y.; Chou, J. H. Water purification by oyster shell bio-medium in a recirculating aquaponic system. *Ecological Engineering [Online]* **2016,** *95*, 229–236.

25. Cheng, G.; Li, Q.; Su, Z.; Sheng, S.; Fu, J. Preparation, optimization, and application of sustainable ceramsite substrate from coal fly ash/waterworks sludge/oyster shell for phosphorus immobilization in constructed wetlands. *Journal of Cleaner Production [Online]* **2018,** *175*, 572–581.

26. Yang, E.-I.; Yi, S.-T.; Leem, Y.-M. Effect of oyster shell substituted for fine aggregate on concrete characteristics: Part I. Fundamental properties. *Cement and Concrete Research [Online]* **2005,** *35* (11), 2175–2182.

27. Yang, E.-I.; Kim, M.-Y.; Park, H.-G.; Yi, S.-T. Effect of partial replacement of sand with dry oyster shell on the long-term performance of concrete. *Construction and Building Materials [Online]* **2010,** *24* (5), 758–765.

28. Da Chen; Zhang, P.; Pan, T.; Liao, Y.; Zhao, H. Evaluation of the eco-friendly crushed waste oyster shell mortars containing supplementary cementitious materials. *Journal of Cleaner Production [Online]* **2019,** *237*, 117811.

29. Chiou, I. J.; Chen, C. H.; Li, Y. H. Using oyster-shell foamed bricks to neutralize the acidity of recycled rainwater. *Construction and Building Materials [Online]* **2014,** *64*, 480–487.

30. Li, G.; Xu, X.; Chen, E.; Fan, J.; Xiong, G. Properties of cement-based bricks with oyster-shells ash. *Journal of Cleaner Production [Online]* **2015,** *91*, 279–287.

31. Teixeira, L. B.; Fernandes, V. K.; Maia, B.; Arcaro, S.; Oliveira, A. N. de. Vitrocrystalline foams produced from glass and oyster shell wastes. *Ceramics International [Online]* **2017,** *43* (9), 6730–6737.

32. Seo, J. H.; Park, S. M.; Yang, B. J.; Jang, J. G. Calcined Oyster Shell Powder as an Expansive Additive in Cement Mortar. *Materials (Basel, Switzerland)* **2019,** *12* (8). DOI: 10.3390/ma12081322.

33. Liu, R.; Da Chen; Cai, X.; Deng, Z.; Liao, Y. Hardened properties of mortar mixtures containing pre-treated waste oyster shells. *Journal of Cleaner Production [Online]* **2020,** *266*, 121729.

34. Her, S.; Park, T.; Zalnezhad, E.; Bae, S. Synthesis and characterization of cement clinker using recycled pulverized oyster and scallop shell as limestone substitutes. *Journal of Cleaner Production [Online]* **2021,** *278*, 123987.

35. Lee, C. H.; Lee, D. K.; Ali, M. A.; Kim, P. J. Effects of oyster shell on soil chemical and biological properties and cabbage productivity as a liming materials. *Waste management (New York, N.Y.) [Online]* **2008,** *28* (12), 2702–2708.

36. Kwon, Y. T.; Lee, C. W.; Yun, J. H. Development of vermicast from sludge and powdered oyster shell. *Journal of Cleaner Production [Online]* **2009,** *17* (7), 708–711.

37. Ok, Y. S.; Oh, S.-E.; Ahmad, M.; Hyun, S.; Kim, K.-R.; Moon, D. H.; Lee, S. S.; Lim, K. J.; Jeon, W.-T.; Yang, J. E. Effects of natural and calcined oyster shells on Cd and Pb immobilization in contaminated soils. *Environ Earth Sci [Online]* **2010,** *61* (6), 1301–1308.

38. Nakatani, N.; Takamori, H.; Takeda, K.; Sakugawa, H. Transesterification of soybean oil using combusted oyster shell waste as a catalyst. *Bioresource technology [Online]* **2009,** *100* (3), 1510–1513.

39. Jeon, J. H.; Son, Y. H.; Kim, D. G.; Kim, T. J. Estimation of Life Cycle CO2 emissions using oyster shells and bottom ash as materials for soil-mixing and a drainage layer. *Journal of Cleaner Production [Online]* **2020,** *270*, 122477.

40. Lee, M.; Tsai, W.-S.; Chen, S.-T. Reusing shell waste as a soil conditioner alternative? A comparative study of eggshell and oyster shell using a life cycle assessment approach. *Journal of Cleaner Production [Online]* **2020,** *265*, 121845.

41. Yang, Y.; Yao, Q.; Pu, X.; Hou, Z.; Zhang, Q. Biphasic calcium phosphate macroporous scaffolds derived from oyster shells for bone tissue engineering. *Chemical Engineering Journal [Online]* **2011,** *173* (3), 837–845.

42. Wu, S.-C.; Hsu, H.-C.; Hsu, S.-K.; Tseng, C.-P.; Ho, W.-F. Preparation and characterization of hydroxyapatite synthesized from oyster shell powders. *Advanced Powder Technology [Online]* **2017,** *28* (4), 1154–1158.

43. Diaz-Rodriguez, P.; Garcia-Triñanes, P.; Echezarreta López, M. M.; Santoveña, A.; Landin, M. Mineralized alginate hydrogels using marine carbonates for bone tissue engineering applications. *Carbohydrate polymers [Online]* **2018,** *195*, 235–242.

44. Wan, M.; Qin, W.; Lei, C.; Li, Q.; Meng, M.; Fang, M.; Song, W.; Chen, J.; Tay, F.; Niu, L. Biomaterials from the sea: Future building blocks for biomedical applications. *Bioactive Materials [Online]* **2021,** *6* (12), 4255–4285.

45. Jong-Hyeon Jung; Kyung-Seun Yoo; Hyun-Gyu Kim; Hyung-Keun Lee; Byung-Hyun Shon. Reuse of Waste Oyster Shells as a SO2/NOx Removal Absorbent. *J. Ind. Eng. Chem [Online]* **2007,** *13*, 512–517.

46. Jairam, S.; Kolar, P.; Sharma-Shivappa, R.; Osborne, J. A.; Davis, J. P. KI-impregnated oyster shell as a solid catalyst for soybean oil transesterification. *Bioresource technology [Online]* **2012,** *104*, 329–335.

47. Xiong, X.; Cai, L.; Jiang, Y.; Han, Q. Eco-Efficient, Green, and Scalable Synthesis of 1,2,3-Triazoles Catalyzed by Cu(I) Catalyst on Waste Oyster Shell Powders. *ACS Sustainable Chem. Eng. [Online]* **2014,** *2* (4), 765–771.

48. Inthapanya, X.; Wu, S.; Han, Z.; Zeng, G.; Wu, M.; Yang, C. Adsorptive removal of anionic dye using calcined oyster shells: isotherms, kinetics, and thermodynamics. *Environmental science and pollution research international [Online]* **2017,** *26* (6), 5944–5954.

49. Liu, X.; Dai, J.; Li, W.; Wang, K.; Huang, J.; Li, Q.; Zhan, G. Green Fabrication of Integrated Au/CuO/Oyster Shell Nanocatalysts with Oyster Shells as Alternative Supports for CO Oxidation. *ACS Sustainable Chem. Eng. [Online]* **2019,** *7* (21), 17768–17777.

50. Li, Y.; Huang, P.; Guo, S.; Nie, M. A promising and green strategy for recycling waste oyster shell powder as bio-filler in polypropylene via mycelium-enlightened interfacial interlocking. *Journal of Cleaner Production [Online]* **2020,** *272*, 122694.

51. Liu, X.; Zhan, G.; Wu, J.; Li, W.; Du, Z.; Huang, J.; Sun, D.; Li, Q. Preparation of Integrated CuO/ZnO/OS Nanocatalysts by Using Acid-Etched Oyster Shells as a Support for CO 2 Hydrogenation. *ACS Sustainable Chem. Eng. [Online]* **2020,** *8* (18), 7162–7173.

52. Jung, J.-Y.; Kim, S.; Lee, H.; Kim, K.; Kim, W.; Park, M. S.; Kwon, J.-H.; Yang, J.-W. Use of extracts from oyster shell and soil for cultivation of Spirulina maxima. *Bioprocess and Biosystems Engineering [Online]* **2014,** *37* (12), 2395–2400.

53. Lee, Y. K.; Ahn, S. I.; Chang, Y. H.; Kwak, H. S. Physicochemical and sensory properties of milk supplemented with dispersible nanopowdered oyster shell during storage. *Journal of dairy science [Online]* **2015,** *98* (9), 5841–5849.

54. Evonik Personal Care. *Pickering emulsion face cream (o/w) with AEROSIL® R 816*. Face cream formulation (Accessed at Glenn Corporation).

55. Siebold, A.; Nardin, M.; Schultz, J.; Walliser, A.; Oppliger, M. Effect of dynamic contact angle on capillary rise phenomena. *Colloids and Surfaces A: Physicochemical and Engineering Aspects [Online]* **2000,** *161* (1), 81–87.

56. Binks, B. P.; Lumsdon, S. O. Influence of Particle Wettability on the Type and Stability of Surfactant-Free Emulsions. *Langmuir [Online]* **2000,** *16* (23), 8622–8631.

Graphical Abstract

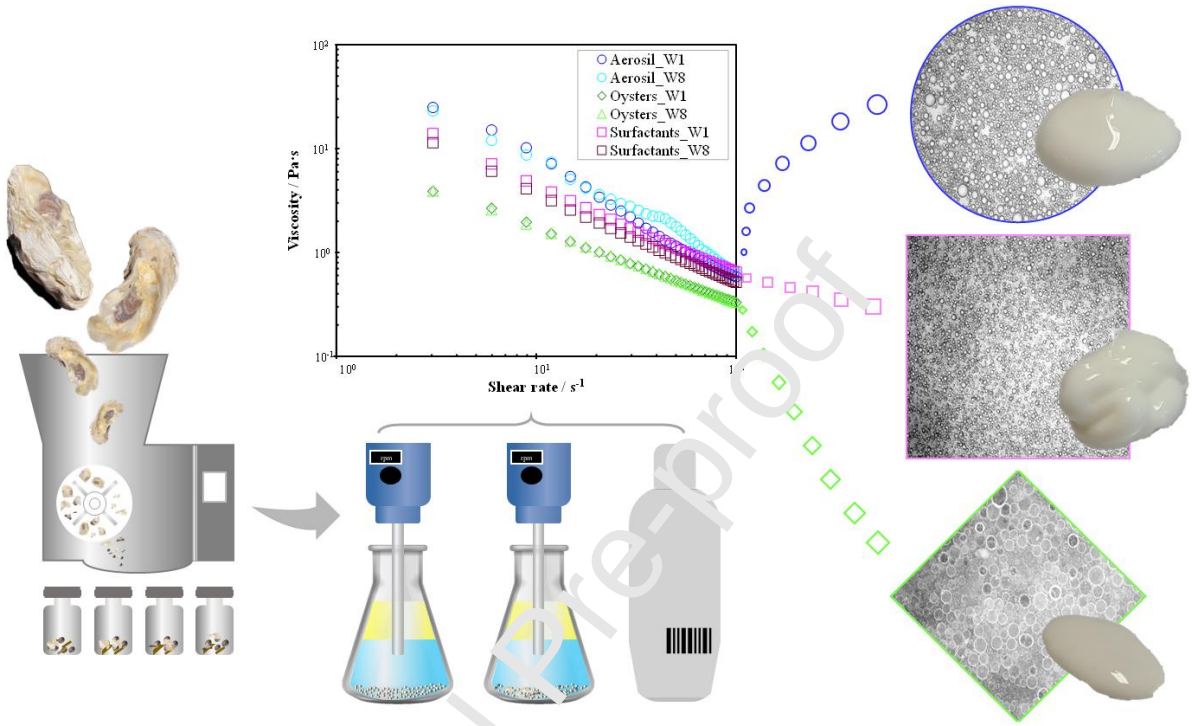

Highlights

- Description of applications suggested for waste oyster shells in different sectors
- Grinding experiments for oyster shells performed with four different types of mills
- Characterization of the physicochemical properties of the grinded fractions including size, shape and surface interactions
- Proposition of an innovative application for oyster shells as emulsion stabilizers
- Rheological analysis to support suitability of the particles as stabilizers